HHS Public Access

Author manuscript

Circ Cardiovasc Imaging. Author manuscript; available in PMC 2017 December 01.

Published in final edited form as:

Circ Cardiovasc Imaging. 2016 December ; 9(12): . doi:10.1161/CIRCIMAGING.115.003584.

Characterization of the Changes in Cardiac Structure and Function in Mice Treated With Anthracyclines Using serial Cardiac Magnetic Resonance Imaging

Hoshang Farhad, MD[*], **Pedro V. Staziaki, MD**[*], **Daniel Addison, MD**, **Otavio R. Coelho-Filho, MD, MPH**, **Ravi V. Shah, MD**, **Richard N. Mitchell, MD, PhD**, **Balint Szilveszter, MD**, **Siddique A. Abbasi, MD**, **Raymond Y. Kwong, MD, MPH**, **Marielle Scherrer-Crosbie, MD, PhD**, **Udo Hoffmann, MD, MPH**, **Michael Jerosch-Herold, PhD**, and **Tomas G. Neilan, MD, MPH**

Non-Invasive Cardiovascular Imaging Program and the Cardiovascular Division, Department of Medicine, Brigham and Women's Hospital, Harvard Medical School, Boston, MA (HF, SAA, RVS, RYK); Cardiac MR PET CT Program, Division of Radiology, Massachusetts General Hospital (PVS, DA, BS, UH, TGN); Department of Pathology, Brigham and Women's Hospital, Harvard Medical School, Boston, MA (RNM); Division of Cardiology, Department of Medicine, Massachusetts General Hospital, Harvard Medical School, Boston, MA (MSC, TGN); Department of Radiology, Brigham and Women's Hospital, Harvard Medical School, Boston, MA (MJH)

Abstract

Background—Anthracyclines are cardiotoxic; however, there are limited data characterizing the serial changes in cardiac structure and function after anthracyclines. The aim of this study was to use cardiac magnetic resonance (CMR) to characterize anthracycline-induced cardiotoxicity (AIC) in mice.

Methods and Results—This was a longitudinal CMR and histological study of 45 wild-type male mice randomized to doxorubicin (DOX, n=30, 5 mg/kg of DOX/week for 5 weeks) or placebo (n=15). A CMR was performed at baseline and at 5, 10 and 20 weeks after randomization. Measures of primary interest included left ventricular ejection fraction (LVEF), myocardial edema (multi-echo short-axis spin-echo acquisition) and myocardial fibrosis (Look-Locker gradient-echo). In DOX-treated mice vs. placebo, there was an increase in myocardial edema at 5 weeks (T2 values of 32±4 vs. 21±3 msec, $P < 0.05$); followed by a reduction in LVEF (54±6 vs. 63±5%, $P < 0.05$) and an increase in myocardial fibrosis (extracellular volume of 0.34±0.03 vs. 0.27±0.03, $P < 0.05$) at 10 weeks. There was a strong association between the early (5 weeks) increase in edema and the sub-acute (10 weeks) increase in fibrosis ($r = 0.90$, $P < 0.001$). Both the increase in edema and fibrosis predicted the late DOX-induced mortality in mice ($P < 0.001$).

Correspondence to: Tomas G Neilan, MD, MPH, Cardio-Oncology Program, Division of Cardiology, Department of Medicine, Cardiac MR PET CT Program, Department of Radiology, Massachusetts General Hospital. 165 Cambridge St, Boston, MA 02114. Tel: (617) 643-0239; Fax: (617) 724-4152; tneilan@mgh.harvard.edu.

[*]Both authors contributed equally to this work

Disclosures

None.

Conclusions—Our data suggest that, in mice, AIC is associated with an early increase in cardiac edema and a subsequent increase in myocardial fibrosis. The early increase in edema and sub-acute increase in fibrosis are strongly linked and are both predictive of late mortality.

Keywords

magnetic resonance imaging; cardiac fibrosis; cardiac edema; anthracyclines; doxorubicin; cardiomyopathy; cardiotoxicity

Anthracyclines are broad-spectrum chemotherapeutic agents used in the treatment of breast cancer, leukemia, lymphoma, and sarcomas. The use of anthracyclines is limited by their dose-dependent cardiotoxicity.[1] Data suggest that more than 20% of patients develop early LV systolic dysfunction[2] and 10 to 20% develop symptomatic heart failure within 5 years.[3, 4] Once established, anthracycline-induced heart failure is progressive, irreversible, and has a predicted two-year survival of 40%.[5]

Current methods for detection of anthracycline-induced cardiotoxicity (AIC) are limited. The current clinical standard is serial measurement of the left ventricular ejection fraction (LVEF). However, measures of LVEF are usually within the normal range,[6, 7] overlooking the myocyte damage that occurs before the decline in LVEF[8, 9] and leading to the incorrect assumption that cardiac injury is absent. Furthermore, once the LVEF has decreased, more than 40% of patients do not recover their baseline LVEF despite expert treatment.[10]

Pathologically, AIC is characterized by acute cardiac edema and the development of myocardial fibrosis.[11–14] Cardiac magnetic resonance (CMR) imaging is the gold-standard imaging technique for detection and quantification of both edema and fibrosis, however there are limited data validating the role of CMR in characterizing these pathological features of AIC.[15] Therefore, the aim of this study was to test the role of the unique tissue characterization provided by CMR for detection of AIC in a mouse model.

Methods

This was a longitudinal study of 45 wild-type C57BL/6 male mice (Jackson Laboratories, Maine, USA) aged 10–12 weeks randomized to doxorubicin (DOX) (n = 30) and placebo (n = 15). The DOX group received 5 mg/kg of DOX/week for 5 weeks by subcutaneous pellet (Innovative Research of America, Florida, USA); in comparison the control group received placebo at similar intervals. This dose and protocol was chosen based on laboratory experience and efforts to mimic clinic protocols.[16]

The experimental protocol was as described in Figure 1. Key measures of interest included left ventricle (LV) size, LVEF, myocardial edema and the myocardial fibrosis measured at baseline, immediately after the 5th cycle of chemotherapy (within 48 hours), at 10 weeks (5 weeks after cessation of chemotherapy), and, in surviving animals, at 20 weeks (10 weeks after cessation of chemotherapy). Blood pressure was measured in all mice by tail-cuff manometry using a CODA-3 noninvasive blood pressure monitoring system (Kent Scientific, Torrington, Connecticut) as previously described.[17, 18] All experiments were approved by the Institutional Animal Care & Use Committee.

Pathology

Sub-groups of mice had pathological examination for confirmation of AIC, cardiac weight and cardiac fibrosis at pre-specified intervals as detailed in Figure 1.

Electron microscopy—For pathological confirmation of AIC, we used the gold-standard of electron microscopy (EM).[12] Representative myocardial sections from 5 mice per group at the 5-week time-point were fixed in 2.5% glutaraldehyde, 2% paraformaldehyde, and cacodylate buffer, at a pH of 7.4. From these, semi-thin sections were cut from these blocks at 1 μm and stained with toluidine blue for light microscopic examination. Subsequently, ultrathin sections were cut from selected blocks at 80 nm, mounted on 200 mesh copper grids, treated with uranyl acetate and lead citrate, and examined in a JEOL 1010 transmission electron microscope (Tokyo, Japan) to obtain representative electron micrographic images of myocardial ultrastructure.

Histological measurement of cardiac fibrosis—Hearts were fixed in formalin solution for histological analysis as previously described.[17, 19] In brief, sections of 5 μm in thickness were stained with Masson's trichrome and viewed under polarized light using a 20× objective. Fifteen to 20 representative areas were chosen in each heart for collagen volume fraction analysis. The Spectrum Analysis algorithm package and ImageScope analysis software (version 9, Aperio Technologies, Inc., Vista, California) were used. The fraction of collagen volume is calculated by counting the number of pixels occupied by the stained region and dividing this count by the number of pixels occupied by the entire section.

Cardiac weight—Cardiac weight was determined by desiccation and comparison of the pre- vs. post desiccation weight as previously described.[20]

Cardiac Magnetic Resonance Imaging

We performed serial CMR scans on a Bruker 9.4-T CMR imaging platform as previously described.[17–19] In brief, for the CMR study, mice were anesthetized with isoflurane (induction 4% to 5%; maintenance 1% to 2% in oxygen from a precision vaporizer). For the CMR study, mice were placed in a special cradle, with electrocardiographic electrodes attached with tape to a front and back paw using electrode gel to optimize contact.

Conventional CMR measurements—For LV volumes, mass and LVEF calculation, the protocol is built on a self-gated (Bruker intra-gate, for cardiac phase-resolved, respiratory-motion compensated cine imaging) fast gradient-echo fast low angle shot sequence with the following parameters (flip angle, 20°; TR, 8.85 msec; TE, 2.36 msec; matrix, spatial resolution, 0.13 × 0.15 mm) as described.[17–19]

Myocardial edema by CMR—For assessment of myocardial edema, a multi-echo short-axis spin-echo acquisition was performed with 5 spin echo-times (7.8 msec, 15.6 msec, 23.4 msec, 31.2 msec, 39 msec, 46.8 msec). The spin-echo acquisitions were both respiratory- and EKG-gated. The spin-echo parameters were as follows: 1 slice, slice thickness 1.0 mm, inter-slice distance 1.4 mm, matrix 128 × 128, spatial resolution 0.23 × 0.23 mm, 2

averages). A repetition time of 200 ~ 400 msec was used, corresponding to triggering at every second or third cardiac cycles. Images were acquired pre-contrast. For processing of T2 image series, the endocardial and epicardial border of the LV were traced for all echo times. As image quality was best on the mid-LV slice and the extracellular volume (ECV) is measured on the mid-LV slice, all T2 measurements were performed in this slice. To analyze the T2 signal, we used proprietary T2 mapping software. In brief, T2 was determined for each myocardial sector from a non-linear least squares fit of the measured echo-amplitude as a function of echo-time TE to an exponential function with constant offset (d): $Mz(TE) = M0*[\exp(-TE/T2) + d]$. M0 refers to the longitudinal equilibrium magnetization, i.e. the magnetization that would correspond to TE = 0, and d is an empirical offset that depends on imperfections in the refocusing pulse, the echo spacing and the echo-train length.[21] The Marquardt-Levenberg algorithm was used for least-squares fitting, with M0, T2, and d, used as variable parameters, and best-fit estimates for these parameters obtained by minimization of the residual sum of squares.

Myocardial fibrosis by CMR—The calculation of myocardial fibrosis by measurement of the ECV was based on pre- and post-contrast T1 measurements as previously described in both humans and animals.[17, 19, 22] In brief, Gadolinium (0.2 mmol/kg) was diluted in saline solution in a 1:10 ratio and administered by multiple intra-peritoneal injections. Myocardial T1 was measured in a mid-LV slice once before contrast and at least 4 times after contrast using a Look-Locker technique no earlier than 6 minutes after contrast administration. The T1 sequence was an EKG-gated Look-Locker sequence with an adiabatic non-slice-selective inversion pulse (hyperbolic secant inversion pulse) and the following parameters for the Look-Locker gradient-echo read-outs: flip angle, 10°; TR, 2.2 msec; TE, 1.6 msec; in-plane resolution, 0.13 × 0.15 mm, slice thickness, 1 mm; repetition time per segment, 22 msec; number of averages, 6 (pre-contrast) or 4 (post-contrast). Each Look-Locker acquisition was made ≈6 to 8 minutes after a subcutaneous injection of contrast. For 6 myocardial segments and the blood pool, signal intensity was plotted versus time after inversion. T1 values were obtained by nonlinear least-squares fitting of the curves of signal intensity versus time after inversion to an analytic expression for the magnitude of the signal measured during the inversion recovery. T1* was corrected for the radiofrequency pulse effects on the inversion recovery to obtain T1. The reciprocal of T1 (R1=1/T1) was used to plot the myocardial R1 against the R1 in the blood pool. A global myocardial ECV for each animal was then calculated by averaging the 6 myocardial segmental values from the mid-LV short-axis slice.

Statistical analysis

Data is presented as mean ±SD or median (range) if applicable. One of the key hypotheses was that the ECV at 10 weeks would be elevated compared with control mice. We planned on a ratio of 0.5 control mice to each DOX-treated experimental mouse and 5 mice from each group to be sacrificed at week 5 and 10 for histological analysis. In preliminary data the ECV was normally distributed with a standard deviation of 0.035. If the true difference in the experimental and control means was 0.045, we calculated that we would need 28 animals to survive to this time-point. This estimation is using a probability (power) of 0.9. Based on prior work, we anticipated that at 10 weeks the mortality rate among DOX-treated mice would be low at 5–10%. Therefore our initial sample size was 28 mice plus 10 mice

sacrificed at week 5 plus the anticipated 10% mortality rate. We therefore began with a sample size of 45 mice with 15 assigned to the placebo-treated control group and 30 to the DOX-treated group.

Measures of interest were continuous variables. Repeated measures were analyzed using a two-factor ANOVA for repeated measures with treatment and time periods. The primary test was comparing means over time periods and, if significant, differences between time-points were analyzed using Tukey-Kramer multiple comparisons tests. We made both treatment and time comparisons as baseline, 5, 10 and 20 weeks. To describe the relationship between measures, the Pearson correlation was calculated. To assess a possible association between the parameter values and animal mortality, survival rates were calculated and event rates were compared with the Log-Rank test. Data were analyzed using SAS version 9.2 (SAS Institute, Cary, NC). For analyses we considered significance at a two-sided $P < 0.05$.

Results

5-week time point

Pathology—There was pathological evidence of AIC on EM images from DOX-treated mice. These findings included prominent vacuolization, enlarged mitochondria, lightened matrix and fragmented cristae (Figure 2). Also, at the 5-week time-point, there was an expanded extracellular space on EM images and an increase in % of water content of the heart at necropsy (75±1% vs. 79±1%, $P = 0.002$).

Conventional CMR Measures—The Table shows the CMR and physiological variables. At the 5-week time-point, there was no statistical difference between DOX- and saline-treated mice in terms of left ventricular end-diastolic volume (LVEDV), LV mass or LVEF. In the DOX group compared with placebo, LVEDV was 130±13 μL vs. 122±13 μL; LV mass was 99±15 μg vs. 95±20 μg; and LVEF was 58±6% vs. 62±4%.

T2 measures by CMR—On CMR, there was an acute increase in T2 values at 5 weeks in DOX-treated animals as compared with controls (32±4 msec vs. 21±3 msec, $P < 0.001$ for ANOVA, and $P < 0.05$ between groups, Table and Figure 3A). There was a close correlation between the acute change in edema by T2 values on CMR and the change in water weight ($r = 0.79$ and $P = 0.007$, Figure 3B).

Native T1 measures by CMR—On CMR, there was an acute increase in native T1 values at 5 weeks in DOX-treated animals as compared with controls (1448±121 msec vs. 1302±152 msec, $P = 0.03$ for ANOVA, and $P < 0.05$ between groups, Table). There was a correlation between the native T1 values and the change in water weight ($r = 0.71$ and $P = 0.02$, Figure 4) and a correlation between native T1 and T2 (r of 0.33 and $P < 0.001$, Figure 5).

Myocardial fibrosis by CMR—There was no change in ECV using the Look-Locker sequence either from baseline or between DOX-treated animals and controls at 5 weeks (0.27±0.02 vs. 0.26±0.03, Figure 6A). There was no difference in the % fibrosis between

DOX- and placebo-treated animals at 5 weeks (2.9±0.2% vs. 3.0±0.25%, P = 0.45, Figure 6B).

10-week time point

Conventional CMR Measures—At the 10-week time-point, DOX-treated animals had an increased LVEDV (142±12 μL vs. 128±11 μL, P < 0.05) and decreased LVEF (54±6% compared to 63±5%, P < 0.05) in comparison to saline-injected mice. There was no statistical difference between DOX- and saline-treated mice in terms of LV mass (93±13 μg vs. 103±16 μg, Table).

Native T1 measures by CMR—There was no difference between native T1 values at 10 weeks in DOX-treated animals as compared with controls (1384±155 msec vs. 1311±128 msec, P > 0.05 between groups, Table).

T2 measures by CMR—There was no difference in T2 values between DOX- and placebo-treated groups at 10 weeks (22±3 msec vs. 22±3 msec, Figure 3A).

Myocardial fibrosis by CMR—On CMR, there was a sub-acute increase in ECV from baseline between DOX-treated animals and saline-treated controls at 10 weeks (0.34±0.03 vs. 0.27±0.03, P < 0.001 for ANOVA, and P < 0.05 between groups, Figure 6A). Fibrosis on CMR correlated strongly with percentage fibrosis on histology (r = 0.93, P < 0.001, Figure 6C). There was also a strong association between increase in fibrosis at 10 weeks and early increase in edema at 5 weeks (r = 0.90, P < 0.001, Figure 6D).

Mortality

Of the initial 30 mice randomized to the DOX group, 10 were sacrificed at pre-specified time-intervals for histology. Of the remaining DOX-treated mice (n=20), none had died by the 5-week or 10-week time points. By the 20-week time point, 15 of the 20 remaining DOX-treated mice had died. From the control group, 10 mice were sacrificed at pre-specified intervals for histology. From the remaining 5 mice, none had died at the 20-week time interval. Figure 7 shows Kaplan Meier curves with event rates for mortality related to native T1 (Figure 7A), T2/edema (Figure 7B), CMR-measured fibrosis/ECV (Figure 7C) and LVEF (Figure 7D). Both T2 and ECV conferred statistical difference to survival. Although LVEF was reduced at 10 weeks after chemotherapy, there was no difference in survival between groups separated by the median LVEF at 10 weeks.

Discussion

The aim of this study was to test whether CMR could provide a longitudinal characterization of the pathological changes that have been described in AIC. We found that anthracyclines were associated with acute cardiac edema, sub-acute myocardial fibrosis, that the extent of edema and fibrosis were related, and that the extent of the early edema and the sub-acute fibrosis predicted the late DOX-induced animal mortality in mice.

The presence of edema in our mouse model is consistent with findings in cross-sectional pathological studies among patients administered anthracyclines.[11, 14, 23–25] However, due to

the invasive nature of cardiac biopsies, longitudinal clinical histological studies are limited. Therefore, a non-invasive method for characterizing the time course of cardiac edema in AIC may be of use. CMR is the gold-standard imaging technique for detection and quantification of myocardial edema.[26] T2-weighted CMR sequences are sensitive to changes in myocardial water content.[26–28] In this study we measured cardiac edema within 48 hours of chemotherapy and found that there was an acute increase in cardiac edema in mice treated with anthracyclines; the increase was transient and had resolved at the next imaging time-point. Similar increases in signal intensity suggestive of edema have been noted in clinical studies performed acutely after anthracyclines and the acute change in edema has been correlated with the subsequent reduction in LVEF.[29]

Similar to edema, pathological clinical studies have consistently documented the presence of myocardial fibrosis in patients treated with anthracyclines.[11, 24, 30, 31] CMR is the also the gold-standard imaging technique for measurement of myocardial fibrosis. There are two CMR methods for detection of fibrosis, namely late gadolinium enhancement (LGE) and T1 quantification or mapping either alone or combined with the use of an extracellular contrast agent to generate an ECV.[17–19, 32–35] While LGE is ideally suited to detection and quantification of replacement myocardial fibrosis such as that which occurs with a myocardial infarct,[36] the ECV and T1 measurements are ideally suited for detection and qualification of the diffuse myocardial fibrosis such as that which occurs in AIC.[17–19, 22] In retrospective clinical studies, we and others have found that LGE was an infrequent finding among patients treated with anthracyclines.[37, 38] In contrast, diffuse fibrosis by ECV was increased.[22] In this study, we extend these findings and report that there was a sub-acute increase in the ECV at 10 weeks after starting anthracyclines in mice, that there was an association between the increase in ECV by CMR and the increase in histological myocardial fibrosis, that there was an association between the acute increase in edema and the sub-acute increase in the ECV and that both edema and fibrosis predicted the late DOX-induced mortality in mice.

We also tested the role of conventional measurement of cardiac structure and function after anthracyclines in mice and specifically the role of serial measurement of LVEF. CMR is a robust imaging technique for the reliable and reproducible measurement of LVEF[39, 40] and cardiac surveillance with serial measurement of LVEF is recommended among patients treated with anthracyclines.[41] Both baseline LVEF and the reduction of LVEF after anthracyclines therapy have been reported to predict clinical events.[42–44] However, while measurement of LVEF is readily available and a robust marker of outcomes in large populations,[45] it has limitations in the monitoring of AIC. Among patients treated with anthracyclines, the LVEF is usually normal[46] despite pathological evidence of extensive myocyte injury.[8, 47] A decline in LVEF is a late manifestation of AIC.[44] Also, once decreased, the LVEF is minimally reversible,[10] and a decrease in LVEF likely represents extensive myocardial injury beyond the ability of the heart to compensate.[8, 48] In support of this, we found that the LVEF was unchanged acutely after anthracyclines despite CMR evidence of edema and histological evidence of AIC. The LVEF did decrease sub-acutely after anthracyclines at the 10-week time-point, which corresponded to the time at which sub-acute fibrosis was detected. However, we found no relationship between the reduction in LVEF sub-acutely after anthracyclines and the late animal mortality. In contrast, imaging

characteristics focused on the histopathological changes in the myocardium, edema and fibrosis, were both predictive of the late animal mortality.

This study should be interpreted within the context of the study design and has limitations which merit discussion. There is significant variability in the quantity, method of administration and dosing schedule among animal studies testing the effect of anthracyclines on cardiac structure and function in mice. Therefore, these data are only relevant to this model and to mice; however, we believe that this study should form part of the basis of testing in a clinical study the role of the unique tissue characterization provided by CMR in tracking the histological changes consistent with AIC. Also the amount of statistical testing used in our study (including multiple variables and time points) produced an error rate above 0.05. Yet, using a Bonferroni adjustment would have been unlikely to change the interpretation of results for highly significant findings (e.g., $P < 0.001$).

In conclusion, these data suggest that, in mice, anthracyclines cause an acute increase in cardiac edema, a subsequent increase in myocardial fibrosis, and that the acute edema and sub-acute fibrosis are related and both predictive of the late DOX-induced animal mortality. Further research is necessary to fully understand the stepwise pathogenesis of AIC in clinical studies and test the role of edema and fibrosis in the characterization of AIC in patients.

Acknowledgments

Sources of Funding

Dr Neilan is supported by an American Heart Association Fellow to Faculty Grant (12FTF12060588, TGN).

References

1. Lipshultz SE, Colan SD, Gelber RD, Perez-Atayde AR, Sallan SE, Sanders SP. Late cardiac effects of doxorubicin therapy for acute lymphoblastic leukemia in childhood. N Engl J Med. 1991; 324:808–815. [PubMed: 1997853]
2. Bosch X, Rovira M, Sitges M, Domenech A, Ortiz-Perez JT, de Caralt TM, Morales-Ruiz M, Perea RJ, Monzo M, Esteve J. Enalapril and carvedilol for preventing chemotherapy-induced left ventricular systolic dysfunction in patients with malignant hemopathies: The overcome trial (prevention of left ventricular dysfunction with enalapril and carvedilol in patients submitted to intensive chemotherapy for the treatment of malignant hemopathies). J Am Coll Cardiol. 2013; 61:2355–2362. [PubMed: 23583763]
3. Limat S, Demesmay K, Voillat L, Bernard Y, Deconinck E, Brion A, Sabbah A, Woronoff-Lemsi MC, Cahn JY. Early cardiotoxicity of the chop regimen in aggressive non-hodgkin's lymphoma. Ann Oncol. 2003; 14:277–281. [PubMed: 12562656]
4. Jensen BV, Skovsgaard T, Nielsen SL. Functional monitoring of anthracycline cardiotoxicity: A prospective, blinded, long-term observational study of outcome in 120 patients. Ann Oncol. 2002; 13:699–709. [PubMed: 12075737]
5. Felker GM, Thompson RE, Hare JM, Hruban RH, Clemetson DE, Howard DL, Baughman KL, Kasper EK. Underlying causes and long-term survival in patients with initially unexplained cardiomyopathy. N Engl J Med. 2000; 342:1077–1084. [PubMed: 10760308]
6. Henderson IC, Allegra JC, Woodcock T, Wolff S, Bryan S, Cartwright K, Dukart G, Henry D. Randomized clinical trial comparing mitoxantrone with doxorubicin in previously treated patients with metastatic breast cancer. J Clin Oncol. 1989; 7:560–571. [PubMed: 2468745]

7. Feher O, Vodvarka P, Jassem J, Morack G, Advani SH, Khoo KS, Doval DC, Ermisch S, Roychowdhury D, Miller MA, von Minckwitz G. First-line gemcitabine versus epirubicin in postmenopausal women aged 60 or older with metastatic breast cancer: A multicenter, randomized, phase iii study. Ann Oncol. 2005; 16:899–908. [PubMed: 15821120]
8. Ewer MS, Ali MK, Mackay B, Wallace S, Valdivieso M, Legha SS, Benjamin RS, Haynie TP. A comparison of cardiac biopsy grades and ejection fraction estimations in patients receiving adriamycin. J Clin Oncol. 1984; 2:112–117. [PubMed: 6699662]
9. Cardinale D, Sandri MT, Martinoni A, Tricca A, Civelli M, Lamantia G, Cinieri S, Martinelli G, Cipolla CM, Fiorentini C. Left ventricular dysfunction predicted by early troponin i release after high-dose chemotherapy. J Am Coll Cardiol. 2000; 36:517–522. [PubMed: 10933366]
10. Cardinale D, Colombo A, Lamantia G, Colombo N, Civelli M, De Giacomi G, Rubino M, Veglia F, Fiorentini C, Cipolla CM. Anthracycline-induced cardiomyopathy: Clinical relevance and response to pharmacologic therapy. J Am Coll Cardiol. 2010; 55:213–220. [PubMed: 20117401]
11. Lefrak EA, Pitha J, Rosenheim S, Gottlieb JA. A clinicopathologic analysis of adriamycin cardiotoxicity. Cancer. 1973; 32:302–314. [PubMed: 4353012]
12. Billingham ME, Mason JW, Bristow MR, Daniels JR. Anthracycline cardiomyopathy monitored by morphologic changes. Cancer Treat Rep. 1978; 62:865–872. [PubMed: 667860]
13. Ferrans VJ. Overview of cardiac pathology in relation to anthracycline cardiotoxicity. Cancer Treat Rep. 1978; 62:955–961. [PubMed: 352510]
14. Unverferth DV, Fetters JK, Unverferth BJ, Leier CV, Magorien RD, Arn AR, Baker PB. Human myocardial histologic characteristics in congestive heart failure. Circulation. 1983; 68:1194–1200. [PubMed: 6640872]
15. Lightfoot JC, D'Agostino RB Jr, Hamilton CA, Jordan J, Torti FM, Kock ND, Jordan J, Workman S, Hundley WG. Novel approach to early detection of doxorubicin cardiotoxicity by gadolinium-enhanced cardiovascular magnetic resonance imaging in an experimental model. Circ Cardiovasc Imaging. 2010; 3:550–558. [PubMed: 20622140]
16. Neilan TG, Jassal DS, Perez-Sanz TM, Raher MJ, Pradhan AD, Buys ES, Ichinose F, Bayne DB, Halpern EF, Weyman AE, Derumeaux G, Bloch KD, Picard MH, Scherrer-Crosbie M. Tissue doppler imaging predicts left ventricular dysfunction and mortality in a murine model of cardiac injury. Eur Heart J. 2006; 27:1868–1875. [PubMed: 16717080]
17. Neilan TG, Coelho-Filho OR, Shah RV, Abbasi SA, Heydari B, Watanabe E, Chen Y, Mandry D, Pierre-Mongeon F, Blankstein R, Kwong RY, Jerosch-Herold M. Myocardial extracellular volume fraction from t1 measurements in healthy volunteers and mice: Relationship to aging and cardiac dimensions. J Am Coll Cardiol. 2013; 6:672–683.
18. Coelho-Filho OR, Shah RV, Mitchell R, Neilan TG, Moreno H Jr, Simonson B, Kwong R, Rosenzweig A, Das S, Jerosch-Herold M. Quantification of cardiomyocyte hypertrophy by cardiac magnetic resonance: Implications for early cardiac remodeling. Circulation. 2013; 128:1225–1233. [PubMed: 23912910]
19. Coelho-Filho OR, Mongeon FP, Mitchell R, Moreno H Jr, Nadruz W Jr, Kwong R, Jerosch-Herold M. Role of transcytolemmal water-exchange in magnetic resonance measurements of diffuse myocardial fibrosis in hypertensive heart disease. Circ Cardiovasc Imaging. 2013; 6:134–141. [PubMed: 23159497]
20. Abdel-Aty H, Cocker M, Meek C, Tyberg JV, Friedrich MG. Edema as a very early marker for acute myocardial ischemia: A cardiovascular magnetic resonance study. J Am Coll Cardiol. 2009; 53:1194–1201. [PubMed: 19341860]
21. Milford D, Rosbach N, Bendszus M, Heiland S. Mono-exponential fitting in t2-relaxometry: Relevance of offset and first echo. PloS one. 2015; 10:e0145255. [PubMed: 26678918]
22. Neilan TG, Coelho-Filho OR, Shah RV, Feng JH, Pena-Herrera D, Mandry D, Pierre-Mongeon F, Heydari B, Francis SA, Moslehi J, Kwong RY, Jerosch-Herold M. Myocardial extracellular volume by cardiac magnetic resonance imaging in patients treated with anthracycline-based chemotherapy. American Journal of Card. 2013; 111:717–722.
23. Friedman MA, Bozdech MJ, Billingham ME, Rider AK. Doxorubicin cardiotoxicity. Serial endomyocardial biopsies and systolic time intervals. JAMA. 1978; 240:1603–1606. [PubMed: 691145]

24. Bernaba BN, Chan JB, Lai CK, Fishbein MC. Pathology of late-onset anthracycline cardiomyopathy. Cardiovasc Pathol. 2010; 19:308–311. [PubMed: 19747852]
25. Zhao Y, McLaughlin D, Robinson E, Harvey AP, Hookham MB, Shah AM, McDermott BJ, Grieve DJ. Nox2 nadph oxidase promotes pathologic cardiac remodeling associated with doxorubicin chemotherapy. Cancer Res. 2010; 70:9287–9297. [PubMed: 20884632]
26. Friedrich MG, Sechtem U, Schulz-Menger J, Holmvang G, Alakija P, Cooper LT, White JA, Abdel-Aty H, Gutberlet M, Prasad S, Aletras A, Laissy JP, Paterson I, Filipchuk NG, Kumar A, Pauschinger M, Liu P. Cardiovascular magnetic resonance in myocarditis: A jacc white paper. J Am Coll Cardiol. 2009; 53:1475–1487. [PubMed: 19389557]
27. Hendel RC, Patel MR, Kramer CM, Poon M, Hendel RC, Carr JC, Gerstad NA, Gillam LD, Hodgson JM, Kim RJ, Kramer CM, Lesser JR, Martin ET, Messer JV, Redberg RF, Rubin GD, Rumsfeld JS, Taylor AJ, Weigold WG, Woodard PK, Brindis RG, Hendel RC, Douglas PS, Peterson ED, Wolk MJ, Allen JM, Patel MR. Accf/acr/scct/scmr/asnc/nasci/scai/sir 2006 appropriateness criteria for cardiac computed tomography and cardiac magnetic resonance imaging: A report of the american college of cardiology foundation quality strategic directions committee appropriateness criteria working group, american college of radiology, society of cardiovascular computed tomography, society for cardiovascular magnetic resonance, american society of nuclear cardiology, north american society for cardiac imaging, society for cardiovascular angiography and interventions, and society of interventional radiology. J Am Coll Cardiol. 2006; 48:1475–1497. [PubMed: 17010819]
28. Abdel-Aty H, Boye P, Zagrosek A, Wassmuth R, Kumar A, Messroghli D, Bock P, Dietz R, Friedrich MG, Schulz-Menger J. Diagnostic performance of cardiovascular magnetic resonance in patients with suspected acute myocarditis: Comparison of different approaches. J Am Coll Cardiol. 2005; 45:1815–1822. [PubMed: 15936612]
29. Wassmuth R, Lentzsch S, Erdbruegger U, Schulz-Menger J, Doerken B, Dietz R, Friedrich MG. Subclinical cardiotoxic effects of anthracyclines as assessed by magnetic resonance imaging-a pilot study. American Heart Journal. 2001; 141:1007–1013. [PubMed: 11376317]
30. Doroshow JH, Tallent C, Schechter JE. Ultrastructural features of adriamycin-induced skeletal and cardiac muscle toxicity. Am J Pathol. 1985; 118:288–297. [PubMed: 3970141]
31. Fedrigo M, Perazzolo M, Frigo A, Cacciavillani L, Corbetti F, Zilio F, Tarantini F, Tona F, Iliceto S, Gambino A, Gerosa G, Thiene G, Angelini A. Abstract 402: Myocardial fibrosis in dilated cardiomyopathy: Comparison between magnetic resonance and histological findings. Circulation. 2009:S335–336.
32. Mewton N, Liu CY, Croisille P, Bluemke D, Lima JA. Assessment of myocardial fibrosis with cardiovascular magnetic resonance. J Am Coll Cardiol. 2011; 57:891–903. [PubMed: 21329834]
33. Neilan TG, Mongeon FP, Shah RV, Coelho-Filho O, Abbasi SA, Dodson JA, McMullan CJ, Heydari B, Michaud GF, John RM, Blankstein R, Jerosch-Herold M, Kwong RY. Myocardial extracellular volume expansion and the risk of recurrent atrial fibrillation after pulmonary vein isolation. JACC Cardiovasc Imaging. 2014; 7(1):1–11. [PubMed: 24290570]
34. Ugander M, Oki AJ, Hsu LY, Kellman P, Greiser A, Aletras AH, Sibley CT, Chen MY, Bandettini WP, Arai AE. Extracellular volume imaging by magnetic resonance imaging provides insights into overt and sub-clinical myocardial pathology. European Heart J. 2012; 33:1268–78. [PubMed: 22279111]
35. Flett AS, Hayward MP, Ashworth MT, Hansen MS, Taylor AM, Elliott PM, McGregor C, Moon JC. Equilibrium contrast cardiovascular magnetic resonance for the measurement of diffuse myocardial fibrosis: Preliminary validation in humans. Circulation. 2010; 122:138–144. [PubMed: 20585010]
36. Kim RJ, Wu E, Rafael A, Chen EL, Parker MA, Simonetti O, Klocke FJ, Bonow RO, Judd RM. The use of contrast-enhanced magnetic resonance imaging to identify reversible myocardial dysfunction. N Engl J Med. 2000; 343:1445–1453. [PubMed: 11078769]
37. Neilan TG, Coelho-Filho OR, Pena-Herrera D, Shah RV, Jerosch-Herold M, Francis SA, Moslehi J, Kwong RY. Left ventricular mass in patients with a cardiomyopathy after treatment with anthracyclines. American Journal of Card. 2012; 110:1679–1686.
38. Tham EB, Haykowsky MJ, Chow K, Spavor M, Kaneko S, Khoo NS, Pagano JJ, Mackie AS, Thompson RB. Diffuse myocardial fibrosis by t1-mapping in children with subclinical

anthracycline cardiotoxicity: Relationship to exercise capacity, cumulative dose and remodeling. J Cardiovasc Magn Reson. 2013; 15:48. [PubMed: 23758789]

39. Armstrong GT, Plana JC, Zhang N, Srivastava D, Green DM, Ness KK, Daniel Donovan F, Metzger ML, Arevalo A, Durand JB, Joshi V, Hudson MM, Robison LL, Flamm SD. Screening adult survivors of childhood cancer for cardiomyopathy: Comparison of echocardiography and cardiac magnetic resonance imaging. J Clin Oncol. 2012; 30:2876–2884. [PubMed: 22802310]
40. Hundley WG, Bluemke DA, Finn JP, Flamm SD, Fogel MA, Friedrich MG, Ho VB, Jerosch-Herold M, Kramer CM, Manning WJ, Patel M, Pohost GM, Stillman AE, White RD, Woodard PK. Accf/acr/aha/nasci/scmr 2010 expert consensus document on cardiovascular magnetic resonance: A report of the american college of cardiology foundation task force on expert consensus documents. Circulation. 2010; 121:2462–2508. [PubMed: 20479157]
41. Ritchie JL, Bateman TM, Bonow RO, Crawford MH, Gibbons RJ, Hall RJ, O'Rourke RA, Parisi AF, Verani MS. Guidelines for clinical use of cardiac radionuclide imaging. Report of the american college of cardiology/american heart association task force on assessment of diagnostic and therapeutic cardiovascular procedures (committee on radionuclide imaging), developed in collaboration with the american society of nuclear cardiology. J Am Coll Cardiol. 1995; 25:521–547. [PubMed: 7829809]
42. Alexander J, Dainiak N, Berger HJ, Goldman L, Johnstone D, Reduto L, Duffy T, Schwartz P, Gottschalk A, Zaret BL. Serial assessment of doxorubicin cardiotoxicity with quantitative radionuclide angiocardiography. N Engl J Med. 1979; 300:278–283. [PubMed: 759880]
43. Schwartz RG, McKenzie WB, Alexander J, Sager P, D'Souza A, Manatunga A, Schwartz PE, Berger HJ, Setaro J, Surkin L, Setaro J, Wackers FJ Th, Zaret BL. Congestive heart failure and left ventricular dysfunction complicating doxorubicin therapy. Seven-year experience using serial radionuclide angiocardiography. American Journal of Med. 1987; 82:1109–1118.
44. Steinherz LJ, Steinherz PG, Tan CT, Heller G, Murphy ML. Cardiac toxicity 4 to 20 years after completing anthracycline therapy. JAMA. 1991; 266:1672–1677. [PubMed: 1886191]
45. Cintron G, Johnson G, Francis G, Cobb F, Cohn JN. Prognostic significance of serial changes in left ventricular ejection fraction in patients with congestive heart failure. The v-heft va cooperative studies group. Circulation. 1993; 87:VI17–23. [PubMed: 8500235]
46. Watts RG, George M, Johnson WH Jr. Pretreatment and routine echocardiogram monitoring during chemotherapy for anthracycline-induced cardiotoxicity rarely identifies significant cardiac dysfunction or alters treatment decisions: A 5-year review at a single pediatric oncology center. Cancer. 2012; 118:1919–1924. [PubMed: 21882180]
47. Mason JW, Bristow MR, Billingham ME, Daniels JR. Invasive and noninvasive methods of assessing adriamycin cardiotoxic effects in man: Superiority of histopathologic assessment using endomyocardial biopsy. Cancer Treat Rep. 1978; 62:857–864. [PubMed: 667859]
48. Ewer MS, Lenihan DJ. Left ventricular ejection fraction and cardiotoxicity: Is our ear really to the ground? J Clin Oncol. 2008; 26:1201–1203. [PubMed: 18227525]

CLINICAL PERSPECTIVE

We designed this study to test whether the unique tissue characterization provided by cardiac magnetic resonance (CMR) could improve the methods for detection of anthracycline-induced cardiotoxicity (AIC). Anthracyclines are a common chemotherapy drug used in the treatment of cancer. Anthracyclines are associated with the development of congestive heart failure and current most clinical surveillance methods for AIC use repeated measures of the left ventricular ejection fraction (LVEF). However, the LVEF is typically normal despite pathological evidence of cardiac toxicity. The consistent early pathological features on invasive biopsy in AIC are cardiac edema and myocardial fibrosis and these pathological changes occur prior to any change in LVEF. Therefore, we performed this study to test whether the imaging of edema and fibrosis by CMR could provide a non-invasive method for tracking the pathological and histological changes that occur in the myocardium after anthracyclines in mice. The study found that mice treated with anthracyclines had an acute increase in cardiac edema, a subsequent increase in myocardial fibrosis, and that the acute edema and sub-acute fibrosis are related and both predictive of the late chemotherapy-induced animal mortality. We believe that this study will form the basis for testing whether the unique tissue characterization provided by CMR can provide a comprehensive assessment of the pathological changes that occur in the myocardium of patients being treated with anthracyclines. Specifically, this study will support further research testing whether the imaging of edema and fibrosis can provide additive information on cardiac toxicity with anthracyclines.

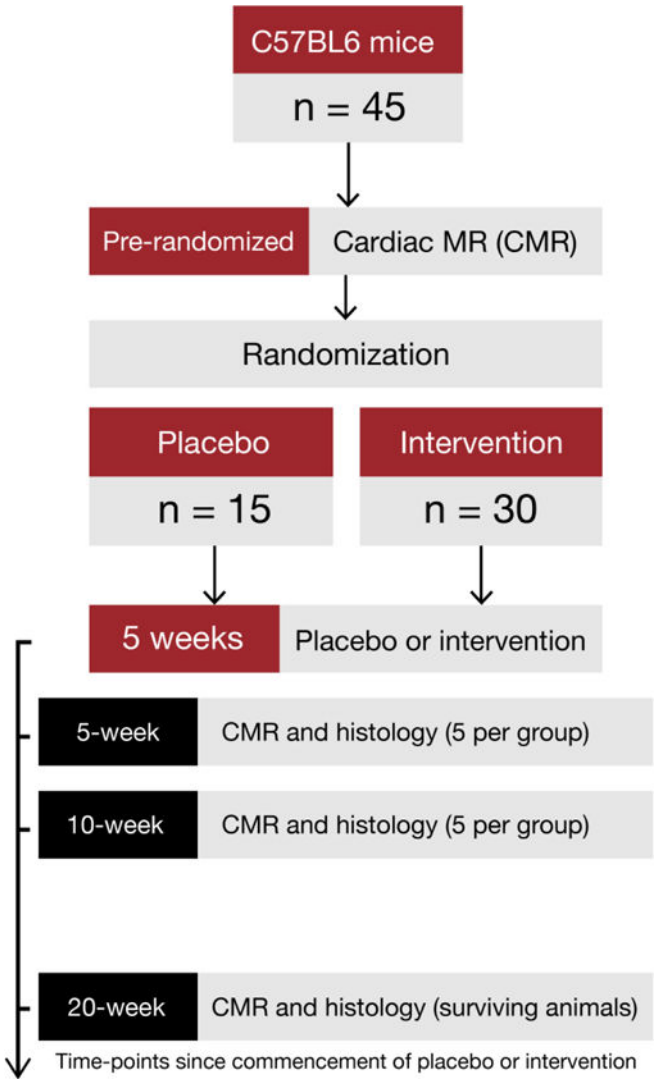

Figure 1.

After baseline CMR imaging, mice were randomized to doxorubicin or placebo. CMR imaging for edema, fibrosis, and function was repeated immediately after 5 weeks from initiation of doxorubicin. At that time a sub-group of mice (n=5 per group) were sacrificed and pathological measurements of myocardial edema and myocardial fibrosis were performed. At 10 weeks (5 weeks after cessation of chemotherapy), mice again underwent a CMR study. At this time-point, another sub-group of mice (n=5 per group) was sacrificed and pathological measurement of myocardial edema and myocardial fibrosis was performed. Remaining mice were followed for mortality and surviving mice were imaged at week 20. After imaging, all mice were sacrificed and histology repeated.

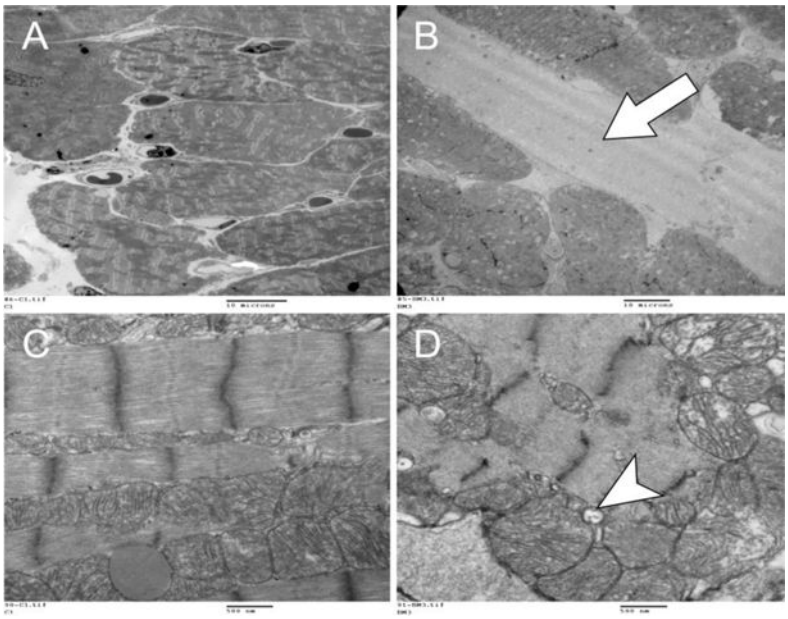

Figure 2.

Representative electron microscopy images of a control (A and C) and doxorubicin-treated (B and D) mouse heart at lower (2,000 ×, A, B) and higher power (30,000 ×, C, D). At lower power, the DOX-treated mouse heart (B) showed an expanded extracellular space (arrow) due to edema in comparison to control (A). At higher power, there is prominent vacuolization (arrow), enlarged mitochondria with lightened matrix and fragmented cristae after DOX (D) in comparison to control with preserved architecture (C). These are all characteristic ultrastructural features of anthracycline toxicity.

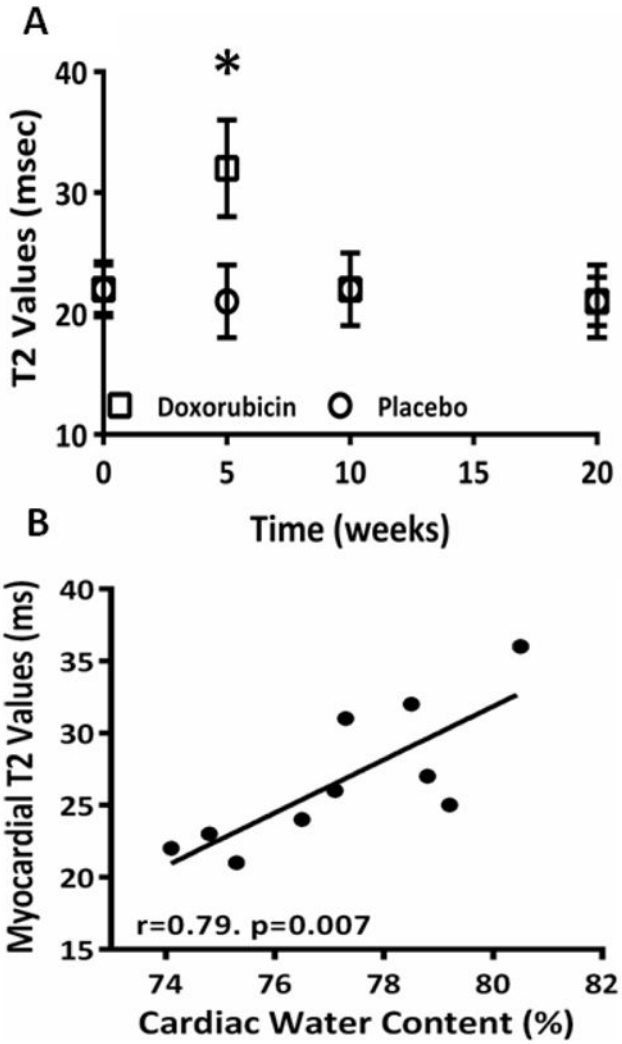

Figure 3.

A) Measurement of cardiac edema using T2-weighted imaging between placebo-treated control mice and DOX-treated mice at baseline, 5 weeks, 10 weeks and 20 weeks showing an increase in cardiac edema in DOX-treated mice at 5 weeks ($P < 0.001$ for ANOVA, * = $P < 0.05$ for between group comparisons); B) Correlation between the CMR-measurement of cardiac edema and cardiac weight.

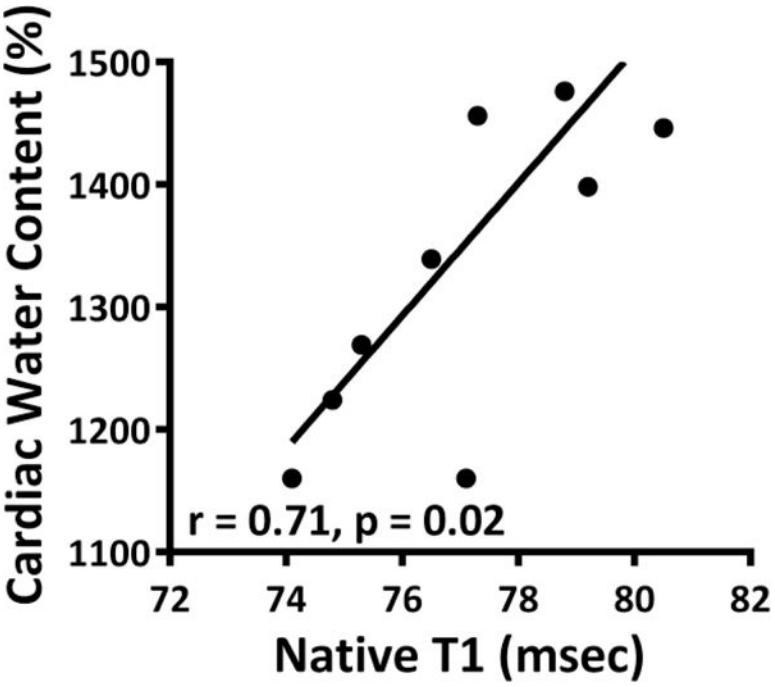

Figure 4.

Comparison of native T1 to cardiac water content revealing a positive correlation between native T1 values and the change in water weight.

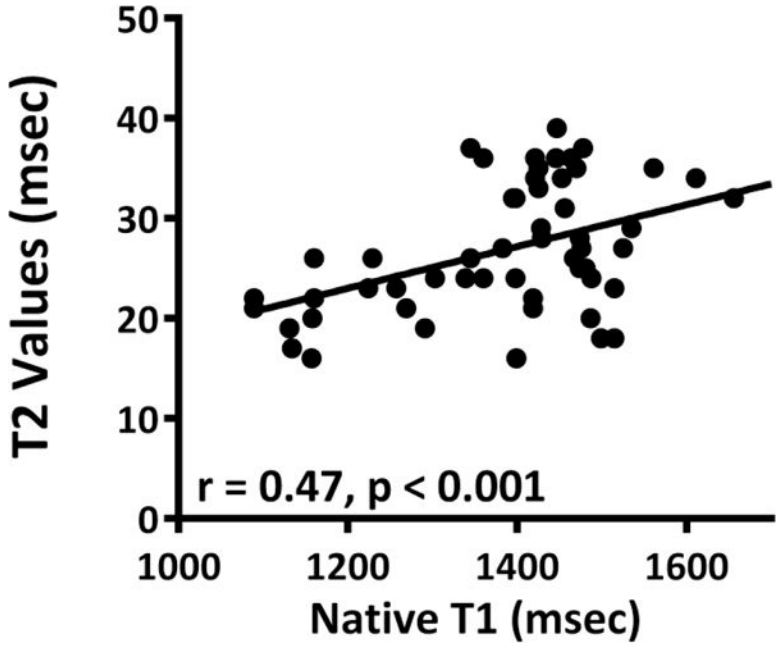

Figure 5.
Comparison of native T1 and T2 values showing a positive correlation between native T1 and T2.

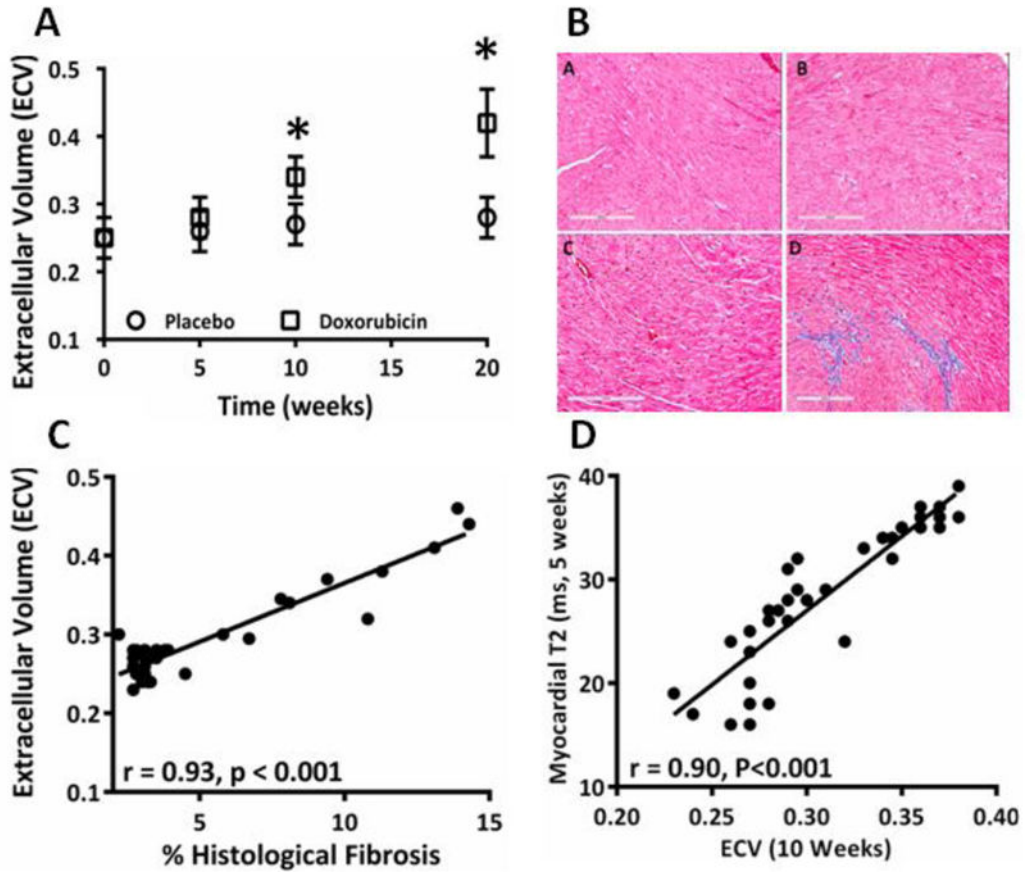

Figure 6.

A) Serial ECV values in DOX-treated and placebo-treated animals over time showing an increase in the ECV at 10 weeks and 20 weeks as compared with the placebo ($P < 0.001$ for ANOVA, * = $P < 0.05$ for between group comparisons); B) Cardiac sections stained with trichrome for detection of fibrosis with representative sections from placebo (a) and DOX-treated (b) mouse at 5 weeks and again at 10 weeks [placebo (c), DOX (d)] showing that myocardial fibrosis did not change at 5 weeks but increased by 10 weeks.

C) There was a strong association between the CMR-measured ECV and the extent of myocardial fibrosis by histology; D) Strong correlation between the early increase in edema at 5 weeks and the subsequent increase in fibrosis by ECV at 10 weeks.

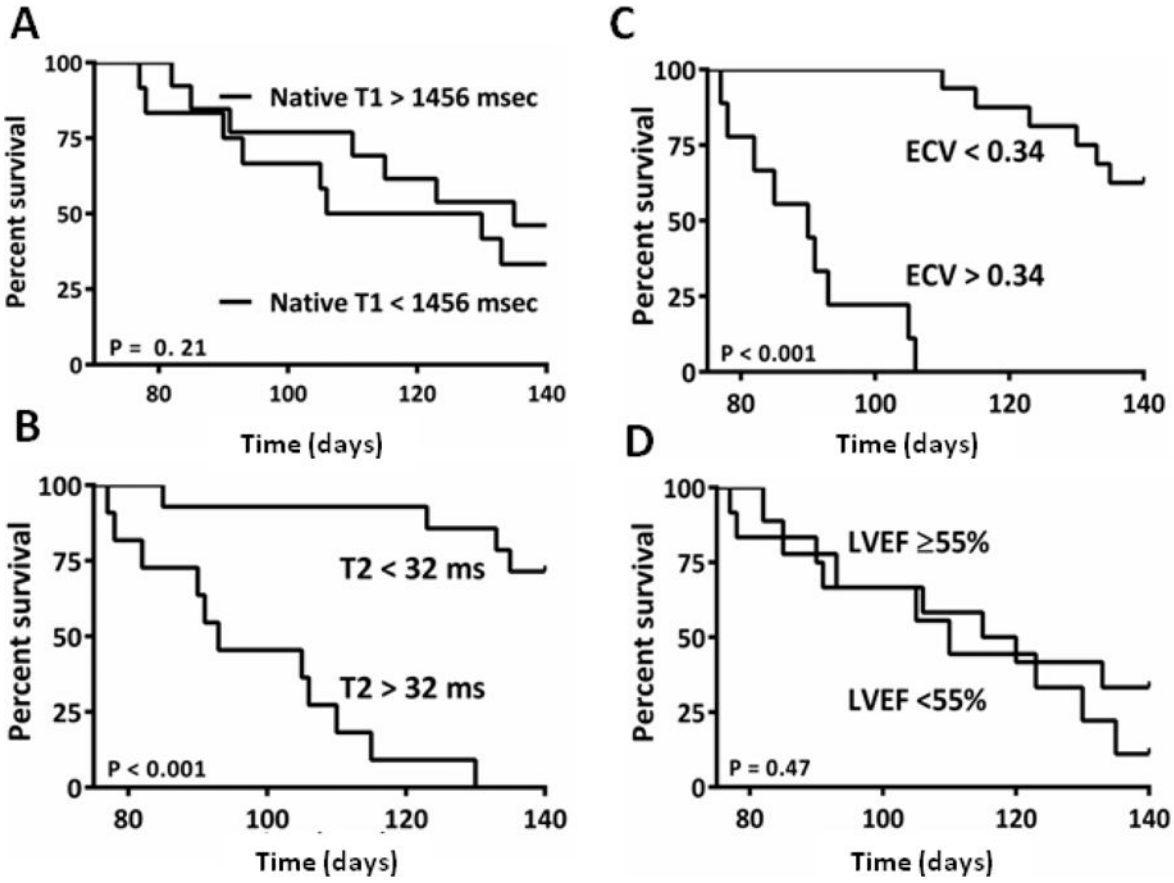

Figure 7.

Figure 5: A) The T1 values were increased at 5 weeks after chemotherapy. Survival curves based on the median measures of cardiac T1 at 5 weeks showing that the early increase in T1 did not predict the DOX-induced mortality; B) The T2 values were increased at 5 weeks after chemotherapy. Survival curves based on the median measures of cardiac edema at 5 weeks showing that the early increase in edema predicted the DOX-induced mortality; C) The ECV was increased at 10 weeks after chemotherapy. Survival curves based on the median measures of the ECV at 10 weeks showing that the intermediate increase in fibrosis predicted the DOX-induced mortality; D) The LVEF was reduced at 10 weeks after chemotherapy. Survival curves based on the median LVEF at 10 weeks showing no difference in animal mortality between mice with an LVEF above and below the median value.

Table

CMR and physiological variables in mice treated with DOX or placebo over time. Comparison of repeated measures was performed using an ANOVA and, if significant, the post-hoc comparison was made using Tukey's comparison test

Variable	HR (per/min)	MAP (mmHg)	LVEDV (μL)	LV Mass (μg)	LV Mass Index (μg/gm)	LVEF (%)	T2 (msec)	Native T1 (msec)	ECV
Baseline									
Placebo	488 ± 25	87±10	110±10	89±12	3.3±0.5	64±3	22±3	1296±158	0.25±0.03
Doxorubicin	490±25	89±9	114±9	89±15	3.3±0.5	63±4	22±3	1318±152	0.25±0.02
5 weeks									
Placebo	498±20	90±9	122±13	95±20	2.9±0.8	62±4	21±3	1302±152	0.26±0.03
Doxorubicin	510±24	80±6*	130±13	99±15	3.6±0.7	58±6	32±4*	1448±121*	0.27±0.03
10 weeks									
Placebo	500±17	92±8	128±11	103±16	2.9±6	63±5	22±3	1311±155	0.27±0.03
Doxorubicin	515±21	83±9	142±12*	93±13	3.0±0.6	54±6*	22±3	1384±128	0.34±0.03*
20 weeks									
Placebo	511±16	97±8	132±11	111±18	2.8±0.5	63±4	21±3	1329±134	0.28±0.03
Doxorubicin	535±19*	81±6	161±15*	85±10	2.3±0.4	38±6*	21±3	1425±144	0.41±0.06*
P value (ANOVA)	0.03	<0.001	<0.001	0.01	0.48	<0.001	<0.001	0.03	<0.001

* = P < 0.05 for comparison of DOX versus placebo.

CMR = cardiac magnetic resonance; DOX = doxorubicin; ANOVA = analysis of variance; HR = heart rate; MAP = mean arterial pressure; LVEDV = left ventricle end-diastolic volume; LV = left ventricle; LVEF = left ventricular ejection fraction; ECV = extra-cellular volume